Subjective Surfaces: a Geometric Model for Boundary Completion

Alessandro Sarti, Ravi Malladi, and James A. Sethian

Department of Mathematics
and
Lawrence Berkeley National Laboratory
University of California
Berkeley, CA 94720

June 6, 2001

Abstract

We present a geometric model and a computational method for segmentation of images with missing boundaries. In many situations, the human visual system fills in missing gaps in edges and boundaries, building and completing information that is not present. These situations have been widely studied by Gestalt psycologists both in the case of modal and amodal completion. Boundary completion presents a considerable challenge in computer vision, since most algorithms attempt to exploit existing data. A large body of work concerns completion models, which postulate how to construct missing data; these models are often trained and specific to particular images. In this paper, we take the following, alternative perspective: we consider a reference point within an image as given, and then develop an algorithm which tries to build missing information on the basis of the given point of view and the available information as boundary data to the algorithm. Starting from the point of view, a surface is constructed. Then it is evolved with the mean curvature flow in the metric induced by the image untill a piecewise constant solution is reached. We test the computational model to modal completion, amodal completion, texture, photo and medical images. We extend the geometric model and the algorithm to 3D in order to extract shapes from low signal/noise ratio medical volumes. Results in 3D echocardiograpghy and 3D fetal echography are presented.

1 Introduction

If we consider the images in Figure **??** we observe that the human visual system completes the internal objects exploiting the existing sparse data. In the image on the left, a solid triangle in the center of the figure appears to have well-defined contours even in completely homogeneous

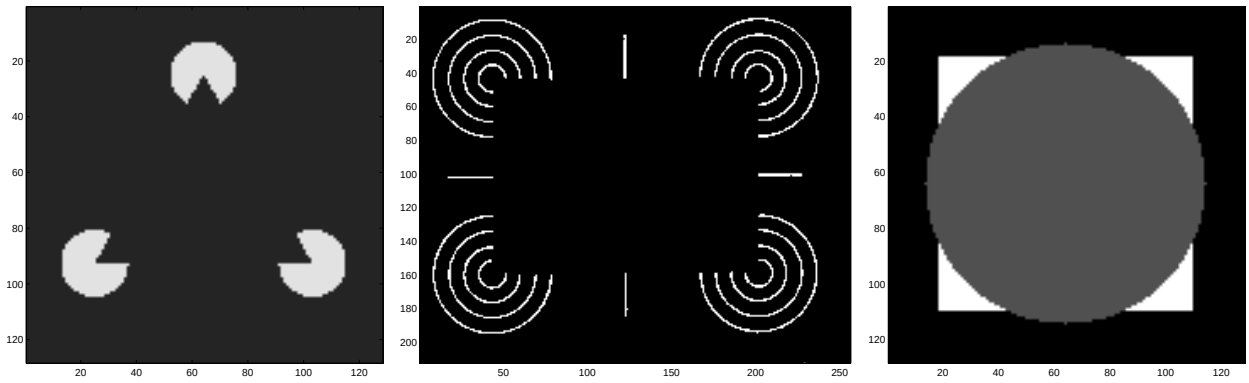

Figure 1: Three images with subjective contours.

areas; in the center figure, a large rectangle is perceived, and, in the figure on the right, a white square partially occluded by a gray disk is perceived. These contours, which are not characterized by image gradients, may be thought of as "apparent" or "subjective" contours. Following the usual convention used in psycology of the gestalt, we distinguish, between "modal completion", in which the goal is to construct a perceived boundary (as in Figure **??**, left and center) and "amodal completion", in which one reconstructs the shape of a partially occluded objects (as in Figure **??**, right); see [**?**, **?**].

Our goal is to extract, i.e. segment, these internal objects. Since some information is missing, one class of algorithms typically complete the segmentation process by building models to postulate what happens between the available data. In this paper we present a method for segmentation of images with missing boundaries.

We take the following perspective:

- The observer is drawn to a reference point within the image, and this is a natural point from which to construct a completion process.
- Starting from this given reference point, we can devise an algorithm which takes advantage of the available boundary data to construct a complete segmentation. Thus, the computed segmentation is a function of the reference point.

As in [**?**], we view a segmentation as the construction of a piecewise constant surface that

varies rapidly across the boundary between different objects and stays flat within it. In [**?**] the segmentation is a piecewise smooth/constant approximation of the image. In our approach the segmentation is a piecewise constant approximation of the point of view- or reference surface. To obtain it we define the following steps:

1. Select a fixation point and build an initial surface corresponding to this point-of-view.
2. Detect existing local features in the image.
3. Evolve the point of view surface with a flow that depends both on the geometry of the surface and on the image features. The flow evolves the initial condition towards a piecewise constant surface. The completed object is the flat mainfold at the top of the surface.
4. (Automatically) Pick the level set that describes the desired object (that is a closed curve).

During the evolution, the point-of-view surface is attracted by the existing boundaries and steepens. The surface evolves towards a piecewise constant solution through the closing of the boundary fragments and the filling in the homogeneous regions. A solid object is delineated as a constant surface bounded by existing and recovered shape boundaries. With this method, the image completion process depends both on the point of view and on the geometric properties of the image [**?**].

The human perceptual organization has been extensively studied by the Gestalt psichologists and their results have been widely used to construct computational models for image segmentation. In particular properties like boundary continuity of direction, regularity, proximity constraints, maximum homogenity, closure, simmetry have been applied as guidelines for many computer vision algorithms. Our geometrical model is inspired also by some experimental results on perceptual organization of the human visual system that have been outlined by Kanizsa [**?**, **?**, **?**]:

1. The emergence of the subjective contours depends on the position of the point of view. In facts "if you fix your gaze on an apparent contour, it disappears, yet if you direct your gaze to the entire figure, the contours appear to be real,"[**?**] pag.48.

2. " The subjective surface is generated by the tendency of the visual system to complete certain figural elements. The contours are therefore the result of perceiving a surface and not viceversa",[?] pag.52.

3. "The completed figure appears to be dislocated in the third dimension and it is perceived as it would be placed "in front" or "above" the other parts of the image"; see [?],pag 275.

4. The emergence of the figure and its illusory boundaries is a direct consequence of the stratification (layering) of the image that is produced by the completion process. [?], pag 278.

In the following we construct a geometrical model for boundary completion by keeping in mind the aforementioned characteristics of perceptual organization. Both the mathematical and algorithmic approach in our method relies on a considerable body of recent work based on a partial differential equations approach to both front propagation and to image segmentation. Level set methods, introduced by Osher and Sethian [?], track the evolution of curves and surfaces, using the theory of curve and surface evolution and the link between between front propagation and hyperbolic conservation laws developed by Sethian in [?, ?]. These methods embed the desired interface as the zero level set of an implicit function, and then employ finite differences to approximate the solution of the resulting initial value partial differential equation. Malladi, Sethian and Vemuri [?] and Caselles, Catte, Coll, and Dibos in [?] used this technology to segment images by growing trial shapes inside a region with a propagation velocity which depends on the image gradient and hence stops when the boundary is reached; thus, image segmentation is transformed into an initial value partial differential equation in which a propagating front stops at the desired edge.

In [?], Sochen, Kimmel, and Malladi view image processing as the evolution of an image manifold embedded in a higher dimensional Riemannian space towards a minimal surface. This framework has been applied to processing both single- and vector-valued images defined in two and higher dimensions (see [?]). In this paper we view segmentation as the evolution of an initial reference manifold under the influence of local image features.

Our approach takes a more general view of the segmentation problem. Rather than follow a particular front or level curve which one attempts to steer to the desired edge (as in [?, ?]), we begin with an initial surface, chosen on the basis of a user-supplied reference fixation point. We then

flow this *entire surface* under speed law dependent on the image gradient, without regard to any particular level set. Suitably chosen, this flow sharpens the surface around the edges and connects segmented boundaries across the missing information. On the basis of this surface sharpening, we can identify a level set corresponding to an appropriate segmented edge.

In [**?**], the theoretical underpinnings of this approach were presented. In this paper we concentrate on results for a variety of 2D images (cognitive, medical, photographic, texture images) and we extend the methodology to the extraction of 3D shapes. In particular we test our algorithm on 2D and 3D medical images in which the signal to noise ratio is truly small and the most part of the edge is missed, as in the case of ultrasound images.

The paper is organized as the following. In Section 2 we review past work in segmentation of images with missing boundaries. In Section 3 we discuss the mathematical problem and in Section 4 we present a numerical method to solve it. In Section 5 the extension of the 2D subjective surface model to 3D manifolds is presented. In section 6 we show results of the application of the method to different 2D images and we discuss both the modal and amodal completion scenarios. In section 7 results of the application of subjective manifolds to 3D image completion are presented and a validation of the method on 3D echocardiographic images is provided. In section 8 a discussion about the accuracy and the efficiency of the computational model is also provided.

2 Past Work and Background

In this section, we review some previous work aimed at recovering subjective contours. We are interested in recovering explicit shape representations that reproduce that of the human visual perception, especially in regions with no image-based constraints such as gradient jump or variation in texture. In Mumford [**?**], the distribution of subjective contours are modeled and computed by particles traveling at constant speeds but moving in directions given by Brownian motion. Williams and Jacobs [**?**, **?**] introduce the notion of a stochastic completion field, the distribution of particle trajectories joining pairs of position and direction constraints, and show how it could be computed. In this approach, a distribution of particles is being computed, rather than an explicit contour/surface, closed or otherwise.

A combinatorial approach is considered in [**?**]. A sparse graph is constructed whose nodes are

salient visual events such as contrast edges and L-type and T-type junctions of contrast edges, and whose arcs are coincidence and geometric configurational relations among node elements. An interpretation of the scene consists of choices among a small set of labels for graph elements. Any given labeling induces an energy, or cost, associated with physical consistency and figural interpretation.

A common feature of both completion fields, combinatorial methods, as well as variational segmentation methods [**?**] is to postulate that the segmentation process is independent of observer's point of focus. On the other hand, methods based on active contours perform a segmentation strongly dependent on the user/observer interaction. Since their introduction in [**?**], deformable models have been extensively used to integrate boundaries and extract features from images. An implicit shape modeling approach with topological adaptability and significant computational advantages has been introduced in [**?**, **?**, **?**]. They use the level set approach [**?**, **?**] to frame curve motion with a curvature dependent speed. These and a host of other related works rely on edge information to construct a shape representation of an object. In the presence of large gaps and missing edge data, the models can go astray and away from the required shape boundary. This behavior is due to a constant speed component in the governing equation that helps the curve from getting trapped by isolated spurious edges. On the other hand, if the constant inflation term is switched off, as in [**?**, **?**], the curve has to be initialized close to the final shape for reasonable results. We also note a more recent segmentation approach introduced in [**?**], in which the authors use geometric curve evolution for segmenting shapes without gradient by imposing a homogeneity constraint. An exaustive review of algorithms for grouping is outside the purpose of this paper. For this concern as well as for the classification of grouping algorithms in the broad families of region-based and contour-based approaches we suggest the interested reader to refer to [**?**].

The approach in this paper rests on view that segmentation, regardless of dimensionality, is a 'view-point' dependent computation[1] The 'view-point' or the user-defined initial guess to the segmentation algorithm serves as input to the algorithm, and is used to construct a point-of-view surface. Next, this reference surface is evolved according to a feature-indicator function. The shape completion aspect relies on two components: (1) the evolution of a surface and (2) a flow

[1]We note, somewhat ironically, that this view of segmentation is in itself 'view-point' dependent.

that combines the effects of level set curve evolution with that of surface evolution. In what follows, we present a geometric framework that makes this possible. Computing the final segmentation (a contour or surface) is accomplished by choosing and plotting a particular level set of a higher dimensional function; as we shall show, this particular level set may be chosen automatically.

3 Theory

3.1 Local feature detection

Consider an image $\mathcal{I} : (x, y) \rightarrow I(x, y)$ as a real positive function defined in some domain $M \subset R^2$. One initial task in image understanding is to build a representation of the local structure of the image. This often involves detection of intensity changes, orientation of structures, T-junctions and texture. The result of this stage is a representation corresponding to *the raw primal sketch* [**?**]. Several methods have been proposed to compute the raw primal sketch, including multiscale/multiorientation image decomposition with Gabor filtering [**?**], wavelet transform [**?**], deformable filter banks [**?**], textons [**?**, **?**] etc. For the purpose of the present paper we consider a simple edge indicator, namely

$$g(x, y) = \frac{1}{1 + (|\nabla G_\sigma(x, y) \star I(x, y)|/\beta)^2} \qquad \text{where} \qquad G_\sigma(\xi) = \frac{\exp(-(\xi/\sigma)^2)}{\sigma\sqrt{\pi}} \tag{1}$$

The edge indicator function $g(x, y)$ is a non-increasing function of $|\nabla G_\sigma(x, y) \star I(x, y)|$, where $G_\sigma(x, y)$ is a gaussian kernel and $(\star)$ denotes the convolution. The denominator is the gradient magnitude of a smoothed version of the initial image. Thus, the value of g is closer to 1 in flat areas ($|\nabla I| \rightarrow 0$) and closer to 0 in areas with large changes in image intensity, i.e. the local edge features. The minimal size of the details that are detected is related to the size of the kernel, which acts like a scale parameter. By viewing g as a potential function, we note that its minima denotes the position of edges. Also, the gradient of this potential function is a force field that always points in the local edge direction; see Figure **??**.

To compute $\nabla G_\sigma(x, y) \star I(x, y)$, we use the convolution derivative property $\nabla G_\sigma(x, y) \star I(x, y) = \nabla(G_\sigma(x, y) \star I(x, y))$ and perform the convolution by solving the linear heat equation

$$\frac{\partial \varphi}{\partial t} = \nabla.(\nabla \varphi) \tag{2}$$

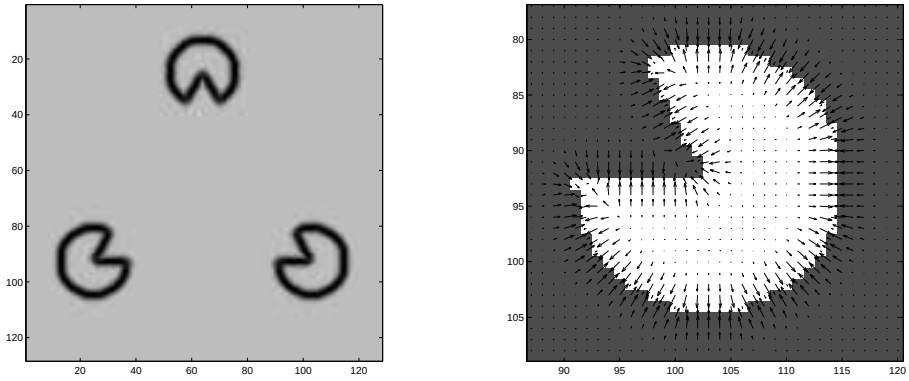

Figure 2: Local edge detection: The edge map g and its spatial gradient $-\nabla g$.

in the time interval $[0, \sigma]$ with the initial condition $\varphi(x, y, 0) = I(x, y)$. We conclude this subsection by observing that there are other ways of smoothing an image as well as computing an edge indicator function or in general a feature indicator function, see, for example, [**?**, **?**, **?**, **?**, **?**, **?**, **?**].

3.2 Global boundary integration

Now, consider a surface $S : (x, y) \longrightarrow (x, y, \Phi)$ defined in the same domain M of the image I. The differential area of the graph S in the Euclidean space is given by:

$$dA = \sqrt{1 + \Phi_x^2 + \Phi_y^2}\; dx\; dy \tag{3}$$

We will use the edge indicator g to stretch and shrink a metric appropriately chosen so that the edges act as attractors under a particular flow. With the metric g applied to the space, we have

$$dA_g = g(x, y)\sqrt{1 + \Phi_x^2 + \Phi_y^2}\; dx\; dy. \tag{4}$$

Now, consider the area of the surface

$$A_g = \int_M g(x, y)\sqrt{1 + \Phi_x^2 + \Phi_y^2}\; dx\; dy, \tag{5}$$

(see Appendix A for derivation) and evolve the surface in order to reduce it. The steepest descent of Eqn. **??** is obtained with usual multivariate calculus techniques and results in the following flow

$$\frac{\partial \Phi}{\partial t} = g\frac{(1 + \Phi_x^2)\Phi_{yy} - 2\Phi_x\Phi_y\Phi_{xy} + (1 + \Phi_y^2)\Phi_{xx}}{1 + \Phi_x^2 + \Phi_y^2} + (g_x\Phi_x + g_y\Phi_y)^2 \tag{6}$$

[2]Note that this is the mean curvature flow in a Riemannian space with conformal metric $g\delta_{ij}$.

See also [**?**] and Appendix B for derivation. The first term on the right hand side is a parabolic term that evolves the surface in the normal direction under its mean curvature weighted by the edge indicator g. The surface motion is slowed down in the vicinity of edges (that is, where $g \to 0$). The second term on the right corresponds to pure passive advection of the surface along the underlying velocity field $-\nabla g$ whose direction and strength depend on position. This term pushes/attracts the surface in the direction of the image edges. Note that $g(I(x,y))$ is not a function of the third coordinate, therefore the vector field $-\nabla g$ lies entirely on the (x,y) plane.

The following characterizes the behavior of the flow (Eqn. **??**):

1. In regions of the image where edge information exists, the edge indicator $g \to 0$ and the main equation **??** reduces to a simple advection equation:

$$\frac{\partial \Phi}{\partial t} \approx g_x \Phi_x + g_y \Phi_y \tag{7}$$

   driving the surface towards the edges. The level sets of the surface also get attracted to the edge and accumulate. Consequently, the spatial gradient increases and the surface begins to develop a discontinuity.

2. Inside homogeneous regions of the image the edge indicator $g = 1$, and the main equation **??** reduces to the euclidean mean curvature flow:

$$\frac{\partial \Phi}{\partial t} = \frac{(1+\Phi_x^2)\Phi_{yy} - 2\Phi_x \Phi_y \Phi_{xy} + (1+\Phi_y^2)\Phi_{xx}}{1+\Phi_x^2+\Phi_y^2} \tag{8}$$

   whose solutions are the orizontal planes characterizing the inside of the figures and the background.

3. We now address the regions in the image corresponding to subjective contours. We take the view that appropriate subjective contours are continuation of existing edge fragments. As discussed above, in regions with well defined edge information, Eqn. **??** causes the level curves to accumulate, thereby causing an increase in the spatial gradient of Φ. Since continuity for the surface is required during the evolution, the edge fragment information is propagated to complete the missing boundary. Now, when spatial derivatives $\Phi_x, \Phi_y \gg 1$, the Eqn. **??**

approximates to

$$\frac{\partial \Phi}{\partial t} \approx g \frac{\Phi_x^2 \Phi_{yy} - 2\Phi_x \Phi_y \Phi_{xy} + \Phi_y^2 \Phi_{xx}}{\Phi_x^2 + \Phi_y^2} + (g_x \Phi_x + g_y \Phi_y). \tag{9}$$

which is commonly taken as the geodesic level set flow [**?**, **?**]. It moves the level curves of the surface towards geodesic curves, meaning towards curves of minimal path connecting existing boundaries. Subjective countours are then straight lines connecting the local features.

4. In regions where $\Phi_x, \Phi_y \ll 1$ Eqn. **??** may be approximated by

$$\frac{\partial \Phi}{\partial t} \approx g(\Phi_{xx} + \Phi_{yy}) + (g_x \Phi_x + g_y \Phi_y). \tag{10}$$

The above equation is non-uniform diffusion equation and denotes the steepest descent of the weighted $L2$ norm, namely

$$\int g |\nabla \Phi|^2 \, dxdy. \tag{11}$$

If the image gradient inside the object is actually equal to zero, then $g = 1$, Eqn. **??** becomes a simple linear heat equation, and the flow corresponds to linear uniform diffusion.

The main equation (Eqn. **??**) is a mixture of two different dynamics, the level set flow (Eqn. **??**) and pure diffusion (Eqn. **??**). Locally, points on the Φ surface move according to one of these mechanisms [**?**]. In steady state solution, the points inside the objects are characterized by pure linear diffusion, while points on the boundary are characterized by the geodesic level set flow. The scaling of the function Φ weights the two dynamics. If Φ contains a narrow range of values, the derivatives are small and the behaviour of the flow (**??**) is mostly diffusive. Conversely, where Φ is contains large variation in values, the behaviour mostly consists of level set plane curve evolution. We perform the scaling by multiplying the initial surface (x, y, Φ_0) (point of view surface) with a scaling factor α.

Remark 1. In the most general case the metric of a Riemannian space is a tensor h_{ij}. In Appendix A we derive the area of a surface embedded in such a manifold. In order to keep mathematically simple our study, we have considered a simple conformal metric $h_{ij} = g\delta_{ij}$. This

metric contains only a scalar information about the local image boundaries. In the general case the tensor metric can be constructed in such a way to contain more information about the local structure of the image like edge direction, color and texture.

Remark 2. In [**?**] the authors associates to the segmentation of an image the following energy functional:

$$E(\Phi, \Gamma) = \lambda^2 \int_{\Omega - \Gamma} |\nabla \Phi|^2 \, dxdy + \mu^2 \int_{\Gamma} d\sigma + \int_{\Omega - \Gamma} (\Phi - I)^2 \, dxdy \tag{12}$$

where Ω is the image domain and Γ is the set of piece-wise smooth boundaries of the objects contained in the image. They look for a minimization of E, that is the smaller E is, the better (Φ, Γ) segments I:

- The first term asks that Φ is almost flat inside the objects, that is in the domain $\Omega - \Gamma$.
- The second term asks that the boundaries Γ that accomplish this be as short as possible.
- The third term asks that Φ approximates I.

Let's consider now the relationship between the subjective surface and the minimization of (**??**).

- Inside of the objects, the subjective surface is flat (driven by the linear diffusion flow), sothat the first integral in (**??**) is identically null.
- The boundaries of the subjective surface are "geodesic" curves, in facts they are driven by the level set geodesic flow, as pointed out in before. They link the existing feature points present in the image with a path of minimal lenght. Then the set of boundary Γ of the subjective surface minimizes the second integral in (**??**)
- The subjective surface is an approximation of the point of view surface and not of the image I, as asked by the third integral in (**??**). Let's point out that the third constrain can be easely matched by initializing $\Phi_0 = I$ in the flow (**??**). Notice that by doing that, models loose the capability to segment objects with the same intensity of the background, as for the Kanitza triangle and most of the images with subjective contours. In the opposite by initializing with the point of view surface means to force the object pointed by the fixing point to pop up *independently from its gray level in the image.*

4 Numerical Scheme and Computational Model

In this section, we show how to approximate Eqn. **??** with finite differences. Let us consider a rectangular uniform grid in space-time (t, x, y); then the grid consists of the points $(t_n, x_i, y_j) = (n\Delta t, i\Delta x, j\Delta y)$. Following standard notation, we denote by Φ_{ij}^n the value of the function Φ at the grid point (t_n, x_i, y_j). We approximate time derivative with a first order forward difference. The first term of Eqn. **??** is a parabolic contribution to the equation of motion and we approximate this term with central differences. The second term on the right corresponds to passive advection along an underlying velocity field ∇g whose direction and strength depend on edge position. This term can be approximated using the upwind schemes. This technique for approximating spatial derivative comes from respecting the appropriate entropy condition for propagating fronts, dicussed in detail in [**?**]. In order to build a correct entropy-satisfying approximation of the difference operator, we exploit the technology of hyperbolic conservation laws. In other words, we check the sign of each component of ∇g and construct one-sided difference approximation to the gradient in the appropriate (upwind) direction [**?**].

With this, we can write the complete first order scheme to approximate equation (**??**) as follows:

$$\Phi_{ij}^{n+1} = \Phi_{ij}^n + \Delta t \left\{ \begin{array}{l} \left[g_{ij} \frac{(1+{D_{ij}^{0x}}^2) D_{ij}^{0yy} - 2 D_{ij}^{0x} D_{ij}^{0y} D_{ij}^{0xy} + (1+{D_{ij}^{0y}}^2) D_{ij}^{0xx}}{1+{D_{ij}^{0x}}^2 + {D_{ij}^{0y}}^2} \right] \\ - \left[\begin{array}{c} [\max(g_{ij}^{0x}, 0) D_{ij}^{-x} + \min(g_{ij}^{0x}, 0) D_{ij}^{+x} \\ + \max(g_{ij}^{0y}, 0) D_{ij}^{-y} + \min(g_{ij}^{0y}, 0) D_{ij}^{+y}] \end{array} \right] \end{array} \right\} \tag{13}$$

where D is a finite difference operator on Φ_{ij}^n, the superscripts $\{-, 0, +\}$ indicate backward, central and forward differences respectively, and the superscripts $\{x, y\}$ indicate the direction of differentiation. We impose Dirichlet boundary conditions by fixing the value on the boundary equal to the minimum value of the point-of-view surface. The time step Δt is upper bounded by the CFL (Courant-Friedrich-Levy) condition that insures the stability of the evolution [**?**].

We summarize the computational steps below:

Segmentation and modal completion of an object with missing boundaries

- First, given an image I, chose a point inside the object (fixation point). Next, build the point-of-view surface Φ_0 by computing the distance function from the fixation point (alternate choice is given in Section 5).
- Compute the edge indicator function g (see Eqn. **??**) corresponding to the given image I.
- Evolve the point-of-view surface towards a piecewise constant solution (subjective surface) according to Eqn. **??**.
- Find the boundary of the segmented object by picking the level set: $\bar{\Phi} = \{\max(\Phi) - \epsilon\}$, for a small $\epsilon > 0$.

Note: Given the edge map g, the only interactive part in the above algorithm is the fixation point choice.

Amodal completion of a partially occluded object

- First, segment the occluding object O_1.
- Build a new edge map $g_{new} = \begin{cases} 1 & (x,y) \in O_1 \\ g & otherwise \end{cases}$
- Use g_{new} to perform modal completion of the partially occluded object

Note: Again, given the edge map g, the only interaction required is the original fixation point choice.

5 3D Subjective Manifolds

In this section we extend the subjective surfaces methodology to the extraction of shapes from volumetric images. Consider a volumetric image $\mathcal{I} : (x, y, z) \to I(x, y, z)$ defined in $M \subset R^3$. As in the 2D case we define a simple edge indicator acting on I

$$g(x,y,z) = \frac{1}{1 + (|\nabla G_\sigma(x,y,z) \star I(x,y,z)|/\beta)^2} \qquad \text{where} \qquad G_\sigma(\xi) = \frac{\exp(-(\xi/\sigma)^2)}{\sigma\sqrt{\pi}}. \quad (14)$$

We now consider a 3-D manifold $V = (x, y, z) \longrightarrow (x, y, z, \Phi(x, y, z))$ defined on the same domain of $\mathcal{I}$. The 3D-manifold is embedded in a 4-D Riemannian space with conformal metric $h_v = g(x, y, z)\delta_{ij}$. Analogous to surface area in the 2D case, we define the volume of the manifold as:

$$V_g = \int_\Omega g\sqrt{1 + \Phi_x^2 + \Phi_y^2 + \Phi_z^2}\; dx\; dy\; dz. \quad (15)$$

See Appendix A for derivation. The minimizing flow for the volume functional is then given by the steepest descent of (**??**), namely

$$\frac{\partial \Phi}{\partial t} = g\frac{(1+\Phi_x^2+\Phi_y^2)\Phi_{zz}+(1+\Phi_x^2+\Phi_z^2)\Phi_{yy}+(1+\Phi_z^2+\Phi_y^2)\Phi_{xx}-2\Phi_x\Phi_z\Phi_{xz}-2\Phi_x\Phi_y\Phi_{xy}-2\Phi_y\Phi_z\Phi_{yz}}{1+\Phi_x^2+\Phi_y^2+\Phi_z^2} + \quad (16)$$
$$g_x\Phi_x + g_y\Phi_y + g_z\Phi_z$$

that is derived with usual multivariate calculus in Appendix B.

The numerical scheme used to approximate Eqn. **??** follows the same line introduced in Paragraph 3.3: we consider a rectangular uniform grid in space-time (t, x, y, z) with the usual grid notation $(t_n, x_i, y_j, z_k) = (n\Delta t, i\Delta x, j\Delta y, k\Delta z)$. As in Eqn. **??**, the parabolic term is approximated by central differences and the advection term is approximated using the upwind schemes. The complete first order scheme to approximate (**??**) is as follows:

$$\phi_{ijk}^{n+1} = \phi_{ijk}^n + \Delta t \left[\begin{array}{c} g_{ijk}\left[\frac{(1+D_{ijk}^{0x^2}+D_{ijk}^{0y^2})D_{ijk}^{0zz}+(1+D_{ijk}^{0x^2}+D_{ijk}^{0z^2})D_{ijk}^{0yy}+(1+D_{ijk}^{0z^2}+D_{ijk}^{0y^2})D_{ijk}^{0xx}}{1+D_{ijk}^{0x^2}+D_{ijk}^{0y^2}+D_{ijk}^{0z^2}}\right. \\ \left. -2\frac{D_{ijk}^{0x}D_{ijk}^{0z}D_{ijk}^{0xz}+D_{ijk}^{0x}D_{ijk}^{0y}D_{ijk}^{0xy}+D_{ijk}^{0y}D_{ijk}^{0z}D_{ijk}^{0yz}}{1+D_{ijk}^{0x^2}+D_{ijk}^{0y^2}+D_{ijk}^{0z^2}}\right] \\ -\left\{ \begin{array}{c} [\max(g_{ijk}^{0x},0)D_{ijk}^{-x} + \min(g_{ijk}^{0x},0)D_{ijk}^{+x} \\ +\max(g_{ijk}^{0y},0)D_{ijk}^{-y} + \min(g_{ijk}^{0y},0)D_{ijk}^{+y} \\ +\max(g_{ijk}^{0z},0)D_{ijk}^{-z} + \min(g_{ijk}^{0z},0)D_{ijk}^{+z}] \end{array} \right\} \end{array} \right] \quad (17)$$

where the same notation of Eqn. **??** has been adopted.